Interference Mitigation Using Uplink Power Control in 5G Relay-Based Heterogeneous Networks

5 authors, including:

Nashwan S A E E D Ghaleb Al-Thobhani
UMS and Sana'a Community College, Yemen, Sana'a

44 PUBLICATIONS   235 CITATIONS

SEE PROFILE

Some of the authors of this publication are also working on these related projects:

Evaluation Study of MPLS Network Potency in YemenNet View project

Extending and Enhancing Data Storage System Based on Blade Server in Telecommunication Company View project

Interference Mitigation Using Uplink Power Control in 5G Relay-Based Heterogeneous Networks

Jamil Sultan[1,2]
[1]Telecommunication Engineering Technology Deptartment
Sana'a Community College
[2]Computer Network Eng. Dept
University of Modern Sceinces
Sana'a, Yemen
jameel730@gmail.com

Waheb A. Jabbar
School of Engineering and Built Environment
Birmingham City University
Birmingham B4 7XG, United Kingdom
waheb.abdullah@bcu.ac.uk

Nashwan S. Al-Thobhani[1,2]
[1]Computer Network Engineering Technology Deptartment
Sana'a Community College
[2]Faculty of Engineering
University of Modern Sciences
Sana'a, Yemen
nashwansg@gmail.com

Abdulaziz Al-Hetar
School of Engineering
Lebanese International University (LIU)
Sana'a, Yemen
alhetar.aziz@ye.liu.edu.lb

Mobarak Saif
Computer Application Programming Dept.
Sana'a Community College
Sana'a, Yemen
mobarak_seif@yahoo.com

Abstract— **Heterogeneous network (HetNet) is an attractive solution for future cellular networks with high data rate and coverage requirements. In HetNets, small cells such as micro cells, pico cells, femto cells and relay node (RN) are added to the network of macro cells in the same region. A large number of low power RNs produces new cell edges with significant intra-cell and inter-cell interferences. In the uplink (UL) scenarios of time-division based HetNets with RN, the user equipment (UE) desired signal may be interfered by the transmissions of the co-channel UEs during the first time slot and by the transmissions of the co-channel UEs or RNs during the second time slot. The interference caused by the RNs may significantly degrade the UE signal. UL transmission power control (PC) is essential for mitigating interference and, as a result, enhancing the cell edge and overall system performance. This research proposes a PC algorithm in order to mitigate the UL interference in 5g relay-based HetNets. This research also investigates the UL performance of HetNets when PC is applied at the RNs. Simulation results indicate that UL PC at the RNs greatly reduces average interference and improves average UL signal-to-interference-plus-noise ratio (SINR) and average UL end-to-end throughput compared to the situation in which UL PC is not implemented.**

Keywords— Power control; 5G; Relay Node (RN); HetNets; Ultra Densification Network (UDN)

I. INTRODUCTION

In recent years, mobile traffic has increased tremendously, mostly as a result of the explosive growth of smart wireless devices and bandwidth-intensive applications [1]. The number of cellular broadband subscribers will increase to 8.8 billion by 2025 [2] and the network's data traffic will reach 351 Exabyte by 2025 [3, 4]. Furthermore, fifth generation (5G) networks are designed to enhance the network capacity by a factor of 1000 times, improve peak data rate 10-100 times, increase the spectral efficiency 5-15 times, reduce latency 10-30 times and achieve 10 times energy efficiency when compared to the 4G networks [5, 6]. Ultra-cell-densification is a major strategy supported by 5G to meet the increased data traffic needs and service requirements [7]. In ultra-cell-densification, operators deploy low cost and low power small cells in the same geographic region of macro cells to form heterogeneous networks (HetNets). The 3rd generation partnership project (3GPP) introduced the HetNet in Release 12 [8]. HetNets include different kinds of small cells with different capabilities. These small cells may be remote radio head (RRH), relay nodes (RNs), micro cells, pico cells and femto cells [7, 9]. HetNet permits these different kinds of small cells to coexist with the macro cells by sharing the same spectrum resources (SRs), which can significantly improve spectral efficiency and reduce uncovered areas. Consequently, there are three spectral sharing strategies in HetNets [6, 10], i.e.,

- **Overlay Spectrum Sharing:** In this strategy, small-cell users (SUs) are allowed to use the SRs that are not used by macro cell users (MUs).

- **Underlay Spectrum Sharing:** In this strategy, the same SRs can be shared between SUs and MUs at the same time. However, the interference power from SUs' transmitters (SUTs) to each MU's receiver (MUR) need to be effectively controlled by introducing a cross-tier interference power constraint.

- **Hybrid Spectrum Sharing:** The SRs are categorized into two types: 1) SRs support high data rate that are only used by SUs, and 2) SRs used by both MUs and SUs (i.e., support high spectrum utilization). The SU with exclusive SRs can attain a higher transmission rate by assigning more transmission power as there is no co-channel interference caused by MUs' transmitters (MUTs). Moreover, the low-rate SUs can share the SRs with MUs to support other communication requirements.

However, the first strategy for spectrum sharing between SUs and MUs is used in this paper. This strategy is chosen in order to make SRs orthogonal within each cell and, hence, eliminate the intra-cell interference. However, the work proposed in this paper can be extended to include the second and third SRs strategies.

Despite the significant advantages of improving the system performance of 5G networks, the deployment of 5G HetNets in practical cases is faced with many challenges [1]. In the HetNets, typical problems include interference, limited energy, backhaul, high costs in small cell deployment and management, handover, spectrum reuse, and limited infrastructure resources. The concurrent operations and the close proximity of neighbouring macro and small cells in the HetNets environment lead to high interferences that limit the user's quality of experience and reduce the current 5G expectations [11]. Furthermore, the level of transmission power of both macro cell and small cell plays an important role in the interference and coverage performance of HetNets [28]. Therefore, the management, mitigation, and cancellation of interferences play a critical part in the current 5G mobile communication [12]. Thus, power control (PC) problem has already received significant attention and has been studied extensively in the literature as the most critical aspect in managing the interference in both uplink (UL) and downlink (DL) of heterogeneous networks [29-33]. In this paper, we propose an UL power control to mitigate the interference and improve the UL performance of 5G relay-based HetNets..

The rest of this paper is structured as follows. A detailed overview of relay-based heterogeneous network is presented in section II. The simulation model is described in Section III. Analysis and discussion of the simulation results are presented in Section IV. Finally, the conclusion of the paper is made in Section V.

II.　Relay-based HetNets

Relaying is a promising technology for next-generation wireless communication that was introduced by 3GPP in Rel-10 [11]. RNs are the least expensive low-power base stations which are usually deployed by operators to provide enhanced coverage and capacity at cell edges, featuring what is considered as wireless backhaul. However, the academic researchers and industrial experts performed extensive researches and as a result they advised that RN can be applied in cellular communication to enhance throughput, energy efficiency, system capacity besides decreasing power consumption [11]. Thus, the future network, which is a combination of different sizes of small cells and RNs networks offers a proliferation of throughput and increases energy and spectral efficiency for both cell-centre and cell-edge users. Also, multi-hopping through various nodes reduces power consumption as well as delay [12]. In relaying, the UEs communicate with the RN, which in turn communicates with a Donor eNB (DeNB) and vice versa.

LTE-Advanced relaying is different to the use of a repeater (Layer 1) that re-broadcasts the signal. The relaying technology in LTE-Advanced is based on layer 3 relay. Layer 3 RN is a decode-and-forward (DF) relay that receives, demodulates and decodes the incoming signal, applies any error correction and then retransmits a new signal [13]. With that processing, both the interference and noise at the backhaul link are eliminated and

a clear signal is transmitted from RN. The layer 3 RNs have unique physical cell IDs different from DeNB and transmit their own synchronization channels, reference symbols and so on. Also, the RN appears to the UEs as a normal eNB that terminates the radio interface and controls its cell [14].

With respect to the resource isolation between access and backhaul links, relay operation for LTE-Advanced can be classified into in-band (Type 1) relaying and out-band (Type 1a). In out-band relaying, the backhaul DeNB-RN link operates on a different carrier frequency utilized by RN-UE radio access for UL and DL [14]. Consequently, full duplex (FD) relay operation can be achieved. In addition, the frequency domain isolation between backhaul and access links results in reduced interference. On the other hand, in in-band relaying, the communication in wireless backhaul between DeNB and RN takes place at the same carrier frequency as the communication in the radio access link between the RN and UE. Therefore, half duplex (HD) relay operation can be realized. However, out-band relaying needs more resource blocks since two channels are required for the access and backhaul links. Due to limited spectrum resources, this technique is completely undesirable, and in-band relay has been the focal point of 3GPP and future wireless communication [15].

In release 10, time-domain separation between access and backhaul links was introduced to achieve the in-band relay operation; which implies that, on the DL carrier frequency at a given time, the RN either transmits on the access link or receives on the backhaul link. Likewise, at a given time on the UL carrier frequency the RN either receives on the access link or transmits on the backhaul link. In the DL, during the first time slot, the base station transmits the signal to the RN and it also sends the signal to the UE directly connected to it. In the second time slot, the RN forwards the transmission to the UE and the base station transmits a new signal to the UE directly connected to it. On the other hand, in the UL, the directly connected user sends the transmission to the base station during the first and second time slots. For the relay users, on the other hand, the user transmits the signal to the RN during the first time slot, whereas the RN forwards the received signal to the base station during the second time slot.

Furthermore, the UE's signal may be interfered by the transmissions of the co-channel UEs during the first time slot whereas it may be interfered by the transmissions of the co-channel UEs or RNs during the second time slot. However, if the interference comes from the co-channel RNs during the second time slot, then the desired UE signal may be severely degraded by the transmissions of the interfering RNs. This is due to the fact that the transmission power of the RNs is higher than the transmission power of the UEs. Hence, UL power control at the RNs is needed in order to mitigate the interference caused by the RNs, thereby allowing the UE to transmit during the second time slot using an modulation and coding scheme (MCS) with spectral efficiency that is near or similar to that of first time slot.

III.　Simulation Model

A. Network Model

A system level simulation implemented in MATLAB is used in this paper to investigate the UL performance of the

interface-limited relay-based HetNets. Seven hexagonal cells with a wrap-around structure [16] is considered for the simulated network. The wrap-round is considered in order to account for the mobility of users particularly on the boundary between two adjacent cell which is called a boundary effect. In each cell, there is one gNB positioned at the centre of the cell in addition to 12 fixed RNs (FRNs) as shown in Fig. 1. In Each cell, 6 RNs are placed between gNB and cell boundary (at $(2/3) \times R$, where R is cell radius) on the line that links the cell's centre to one of the six cell vertices while the other 6 RNs are placed (at $(\sqrt{3}/3) \times R$) on the line that links the cell's centre to the mid of each hexagon's side. The RNs are assumed to be in-band DF layer 3 relays [12]. 30 UEs are deployed randomly in a uniform distribution all over the centre cell and the first and second tier cells. In each simulation iteration, the UEs randomly choose its direction of movement by means of the modified random direction mobility model. At the first simulation iteration, the direction of each UE is chosen randomly using the uniform distribution in the range (0, 360) degrees. After that, each UE is randomly designated a new direction in the range $(-45, 45)$ degrees with respect to its former direction [17]. However, the users in the second tier cells are fixed and the purpose of introducing them is to generate interference to the users of the first tier cells. Meanwhile, the considered traffic model is the full-buffer model in which each UE has data to transmit or receive in the buffer at all times [18]. 5G makes use of time-frequency resource allocation, in which the frequency bandwidth is split into orthogonal units called physical resource blocks (PRBs), each of which is allocated separately. Each user is assigned one PRB, which consists of a group of 12 sub-carriers and the bandwidth of every sub-carrier is 15kHz. The hard handover (HHO) algorithm defined in [19, 20] is considered. The main parameters of the simulation are summarized in Table I [10, 21]. In this simulation, we investigate and compare the UL performance of two scenarios; namely scenario 1 wherein no PC is used at the RNs and scenario 2 in which the PC at the RNs is used. The performance metrics are the average UL signal-to-interference-plus-noise ratio (SINR) and average UL end-to-end (e2e) throughput.
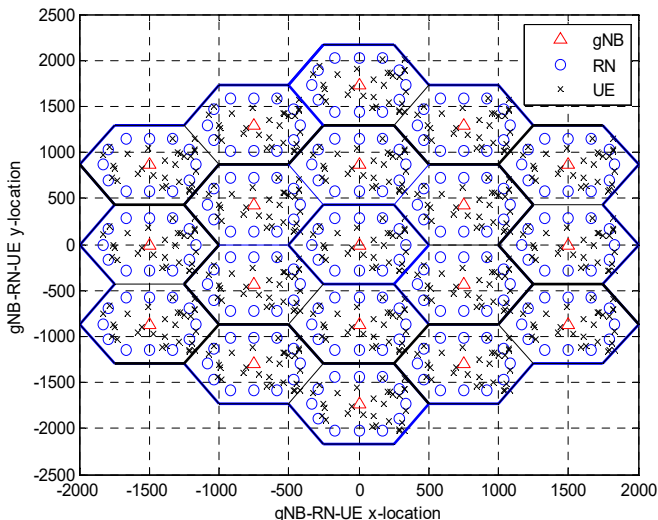

Fig. 1   Simulated cellular layout

Parameter	Value
Cell radius	500 m
Carrier frequency	3.5 GHz
Channel bandwidth	10 MHz
FFT Size	1024
UE distribution	Uniform random distribution
HHO A3 Hysteresis	3 dB
A3 time-to-trigger (TTT)	160 ms
Transmitted power	gNB: 46 dBm, RN: maximum 33 dBm, UE: 23 dBm
Standard deviation of shadowing	Access links: 10 dB, Backhaul links: 4 dB
De-correlation distance of shadowing	25 m
Antenna heights	gNB: 30 m, RN: 15m, UE: 1.5m
UE speed	30 km/hr
Traffic model	Full buffer
Noise figure	gNB & RN: 5 dB, UE: 9 dB

B. Propagation Model

Both macro and small cells in an urban area are considered in our simulation. It is assumed that the backhaul link between the gNB and RN is reliable and in line of sight (LOS), whereas the access links between the gNB and UE and between RN and UE are in non LOS (NLOS). The WINNER II Type 5a and Type 5f path loss models are considered for the backhaul LOS and NLOS links, respectively. In addition, the WINNER II Type C2 model is utilized for calculating the path loss of the access links for both macro and small cell [22, 23] as follows:

$$PL = [44.9 - 6.55\log_{10}(h_{BS})]\log_{10}(d) + 26.46 + 5.83\log_{10}(h_{BS}) + 20\log_{10}\left(\frac{f}{2}\right) \tag{1}$$

where d is the distance between gNBs/RNs and UEs (in meter) with $50m < d < 5km$, h_{BS} is the antenna height of gNB/RN, and f is the carrier frequency in GHz with $2GHz \leq f \leq 6GHz$.

For modeling of the large-scale shadow fading, a lognormal random variable is used, with zero mean and standard deviations for the access links and the backhaul links of 10 dB and 4 dB, respectively. The temporal correlation of the shadowing is taken into account with a decorrelation distance of 25 m.

C. Modeling of the Average UL SINR

It is assumed that all PRBs are assigned in all cells simultaneously. The average UL SINR measured at the gNB/RN of each PRB j for each user k can be written as

$$\bar{\gamma}_{j,k}^{UL} = \frac{P_{k,s}^{j}}{\sum\limits_{i \in \Phi_i} I_{i,s}^{j} + P_N} \tag{2}$$

where $P_{k,s}^{j}$ is the average UL received power of PRB j which takes into consideration the path loss and large-scale shadow fading between the user terminal k and the serving station s, $I_{i,s}^{j}$ is the average interference experienced by user k at its serving station s that is caused by the UEs/RNs of cell i at PRB j, the subscripts s and i denote the serving cell and the interfering cell, respectively, Φ_i is the group of interfering cells and P_N is the power of receiver noise.

D. Modulation and Coding Rate

The average UL SINR measured at the gNB/RN of each PRB j is then quantized into a channel quality indicator (CQI) value indicative of the highest modulation and coding rate the UE may use while keeping a packet error rate (PER) below a target of 10% as shown in Table II [24-26]. The gNB/RN then feeds back these CQI values to the UE.

TABLE II.   SINR AND CQI MAPPING TO MODULATION AND CODING RATE

CQI	Modulation	Code rate (x 1024)	Spectral Efficiency (SE) bits/symbol)	SINR (dB)
1	QPSK	78	0.1523	-6.936
2	QPSK	120	0.2344	-5.147
3	QPSK	193	0.3770	-3.180
4	QPSK	308	0.6016	-1.253
5	QPSK	449	0.8770	0.761
6	QPSK	602	1.1758	2.699
7	16QAM	378	1.4766	4.694
8	16QAM	490	1.9141	6.525
9	16QAM	616	2.4063	8.573
10	64QAM	466	2.7305	10.366
11	64QAM	567	3.3223	12.289
12	64QAM	666	3.9023	14.173
13	64QAM	772	4.5234	15.888
14	64QAM	873	5.1152	17.814
15	64QAM	948	5.5547	19.829

E. Uplink Power Control

When the PC is used at the RN, the RN's UL transmitted power is adjusted so that all RNs achieve the target SINR $(\bar{\gamma}_t)$ according to their channel conditions and encountered interference levels. Hence, the UL transmitted power of the RN r (P_r) can be updated as follows:

$$P_r(m+1) = \begin{cases} P_r^{\max}, & \text{if } X_r(P(m)) > P_r^{\max} \\ P_r^{\min}, & \text{if } X_r(P(m)) < P_r^{\max} \\ X_r(P(m)), & \text{otherwise} \end{cases} \quad (3)$$

where m is the frame index, $P_r^{\max}$ is the maximum RN transmitted power, $P_r^{\min}$ is the minimum RN transmitted power and $X_r(P(m))$ is given by:

$$X_r(P(m)) = \frac{P_r(m)\bar{\gamma}_t}{\bar{\gamma}_{RD,2}(m)} \quad (4)$$

where $P_r(m)$ is the transmitted power of the RN at the mth frame, $\bar{\gamma}_t$ is the target SINR of the R $\rightarrow$ D link and $\bar{\gamma}_{RD,2}(m)$ is the average UL SINR of the R $\rightarrow$ D link at the frame m that can be given by:

$$\bar{\gamma}_{RD,2}(m) = \frac{G_{rc}P_r(m)}{\sum_{i \neq c} I_{ic}(m) + P_N} \quad (5)$$

where G_{rc} is the link gain that captures the effects of the path loss, the shadow fading and the transmitting and receiving antenna gains between RN r and serving gNB of cell c, I_{ic} is the average interference comes from cell i to the gNB of cell c and P_N is the noise power of the gNB of cell c.

F. Average end-to-end (e2e) Throughput

The average e2e throughput for the relay-based transmission can be calculated as [27]:

$$Th_{e2e,R} = \frac{SE(\bar{\gamma}_{SR,1}) \times SE(\bar{\gamma}_{RD,2})}{SE(\bar{\gamma}_{SR,1}) + SE(\bar{\gamma}_{RD,2})} \quad (6)$$

where $SE(\bar{\gamma}_{SR,1})$ is the spectral efficiency for the selected MCS for the source (UE) to RN link during time slot 1, and $SE(\bar{\gamma}_{RD,2})$ is the spectral efficiency for the selected MCS for the RN to destination (gNB) link during time slot 2.

The average e2e throughput of the direct link between source (UE) and destination (gNB) (S→D) can be given by:

$$Th_{e2e,B} = \frac{1}{2}\left(SE(\bar{\gamma}_{SD,1}) + SE(\bar{\gamma}_{SD,2})\right) \quad (7)$$

where $SE(\bar{\gamma}_{SD,i})$ is the spectral efficiency of the MCS selected for the source (UE) to destination (gNB) link during time slot i and the factor $\frac{1}{2}$ accounts for the fact that two time slots with equal duration is needed in this case.

IV. SIMULATION RESULTS AND DISCUSSIONS

Fig. 2 shows the average UL interference experienced by UE during the first and the second time slots for the scenario 1 and scenario 2. It's obvious from this figure that for scenario 1 without PC the interference during the second time slot is higher than the interference during the first time slot. This is because the interference during the second time slot is caused by the UEs and/or RNs of other co-channel cells. On the other hand, the interference during the first time slot is caused by the UEs of other cells only. In fact, in scenario 1 the average UL interference during the first time slot is $-82.4\,dB$ whereas the average UL interference during the second time slot is $-72.2\,dB$. It is also noted from Figure 1 that for scenario 2 with PC the average UL interference during the first and second time slots are almost the same and equals -82.4 dB. This is because of

using PC at the RNs that reduces RNs' UL transmitted power and hence reducing UL interference during second time slot.
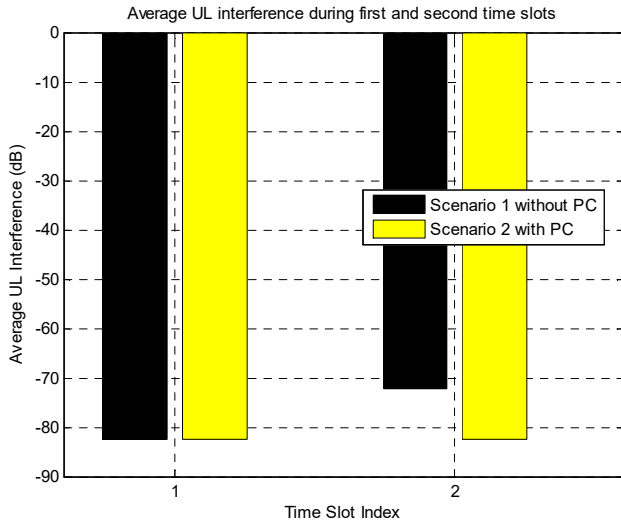

Fig. 2   Average UL interference during the first and second time slots for both scenarios

Fig. 3 depicts the cumulative distribution function (CDF) of the average UL e2e throughput for all users (users of RNs and users of gNBs) for the two simulated scenarios. As shown in the figure, the average UL e2e throughput for scenario 2 with PC is better than that of scenario 1 without PC. However, 50% of the average UL e2e throughput is higher than 1.093 bps/Hz in scenario 1 whereas it is higher than 1.406 bps/Hz in scenario 2. The average UL e2e throughput for scenario 2 is better by 28.6% than the scenario 1.
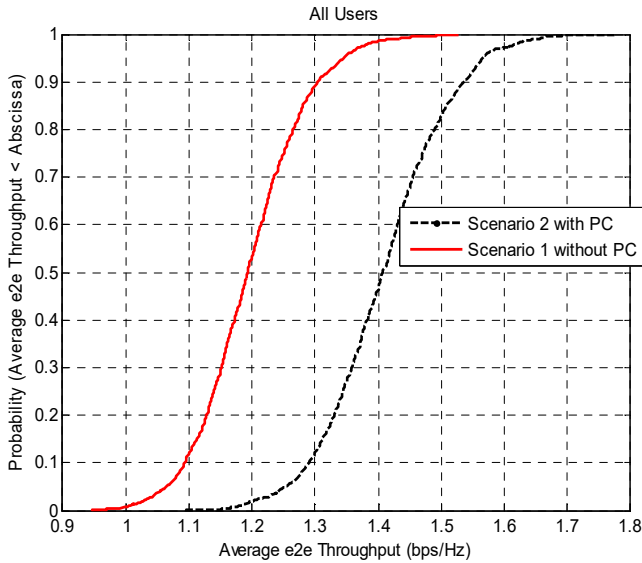

Fig. 3   CDF of average UL e2e throughput for both scenarios for all UEs

Fig. 4. depicts the CDF of the average UL e2e throughput for the two simulated scenarios considering only the UEs connected with macro gNBs. The reason for considering the UEs connected with gNBs as their serving station is that those users are affected by the interference caused by the RNs during

the second time slot and hence their performance are significantly enhanced when the transmission power of the RNs is reduced due to the use of PC. As shown in the figure, the average UL e2e throughput for scenario 2 with PC is significantly better than that of scenario 1 without PC. However, in scenario 1, 50% of the average UL e2e throughput is higher than 1.764 bps/Hz whereas it is higher than 2.481 bps/Hz in scenario 2. The average UL e2e throughput for scenario 2 is better by 40.6% than the scenario 1.
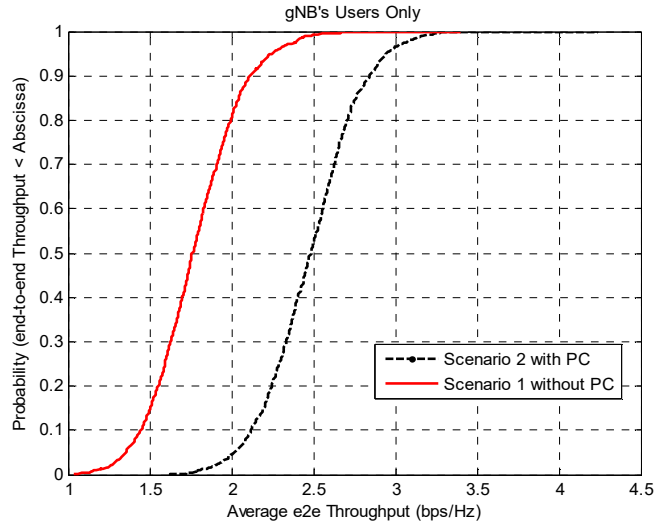

Fig. 4   CDF of Average UL e2e throughput for both scenarios for gNBs' UEs only

Fig. 5. depicts the CDF of the average UL SINR for both scenario 1 and 2. In this figure, only the users of gNBs are considered. It is clear from this figure that scenario 2 with PC achieves higher UL SINR compared to scenario 1 without PC. In fact, 50% of the average UL SINR is higher than 3.055 dB in scenario 1 while 50% of the average UL SINR is higher than 8.202 dB in scenario 2. Hence, for users connected with gNBs, using PC in scenario 2 improves the UL SINR by 168.48% compared to that of scenario 1 without PC. This is due to the fact that users of gNBs are greatly affected by the interference caused by RNs during the second time slot. Hence, using PC at the RN will decrease RNs' transmitted power which results in reducing the interference during the second time slot and improving the SINR performance of the UEs connected to gNBs.

Fig. 6 illustrates the average UL SINR for gNBs' UEs only at different values of the target UL SINR $(\bar{\gamma}_t)$ required at the $R \rightarrow D$ link. It is obvious from this figure that the proposed scenario 2 with PC significantly outperforms scenario 1 without PC at the different values of $\bar{\gamma}_t$. However, as the required SINR in the $R \rightarrow D$ link $(\bar{\gamma}_t)$ increases, the performance difference between scenario 1 and scenario 2 decreases. This is because of that at low values of $\bar{\gamma}_t$, the PC algorithm significantly decreases the RNs' transmitted power to meet the small value of $\bar{\gamma}_t$ which results in lower interference during second time slot. On the other hand, when the target UL SINR in $R \rightarrow D$ link increases, the UL PC algorithm increases the RNs' transmitted

power in order to satisfy the required $\bar{\gamma}_t$ in which case the UL interference during the second time slot is increased and the hence the UL SINR is decreased. In fact, at $\bar{\gamma}_t = 5dB$, the average UL SINR for scenario 1 and 2 are 8.081 dB and 2.897 dB, respectively. On the contrary, at $\bar{\gamma}_t = 30dB$, the average UL SINR for scenario 1 and 2 are 6.187 dB and 2.897 dB, respectively. However, at $\bar{\gamma}_t = 40dB$, both scenarios 1 and 2 achieve the same UL SINR. This is because of the high $\bar{\gamma}_t$ that makes RNs in scenario 2 transmit using high transmitted power that is similar or near to the transmitted power used in scenario 1 without PC.
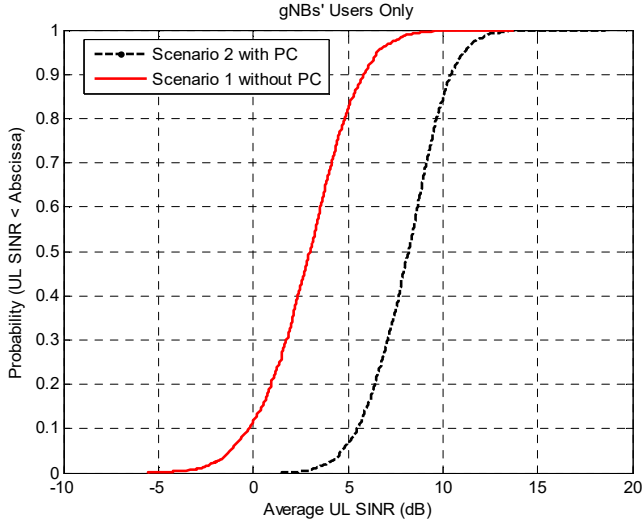

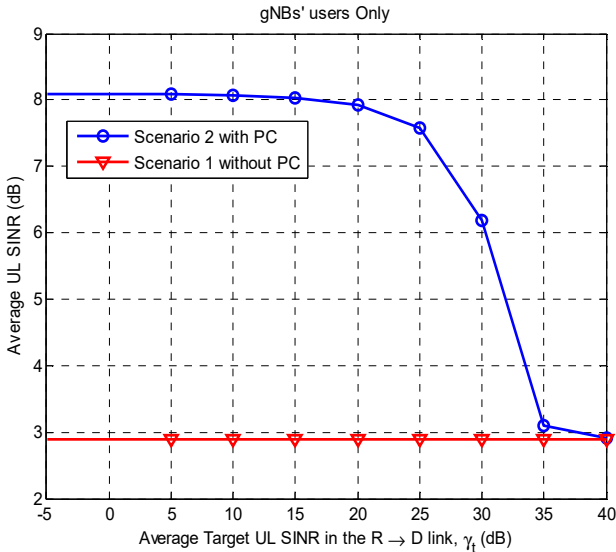Fig. 5   CDF of Average UL SINR for gNB's users only

Fig. 6   Average UL SINR for gNBs' UE only at different value of the UL SINR required in the $R \rightarrow D$ link, $\bar{\gamma}_t$

Fig. 7 shows the average UL e2e throughput for gNBs' UE only at different values of the target UL SINR $(\bar{\gamma}_t)$ required at the backhaul $R \rightarrow D$ link. It is obvious from this figure that the

proposed scenario 2 with PC significantly outperforms scenario 1 without PC at the different values of $\bar{\gamma}_t$. However, as the required SINR in the $R \rightarrow D$ link $(\bar{\gamma}_t)$ increases, the difference in the average UL e2e throughput between scenario 1 and scenario 2 decreases. In fact, at $\bar{\gamma}_t = 5dB$, the average UL e2e throughput for scenarios 1 and 2 are 2.482 bps/Hz and 1.778 bps/Hz, respectively. On the contrary, at $\bar{\gamma}_t = 30dB$, the average UL e2e throughput for scenarios 1 and 2 are 2.139 bps/Hz and 1.778 bps/Hz, respectively. However, at $\bar{\gamma}_t = 40dB$, both scenarios 1 and 2 achieve the same UL e2e throughput. It should also be noted that the average UL e2e throughput for scenario 1 is constant as $\bar{\gamma}_t$ increases. This is because of the fixed RNs transmitted powers used in scenario 1 which results in fixed UL interference caused by RNs to the gNBs' UEs during the second time slot which therefore leads to fixed UL e2e throughput for gNBs' UEs.
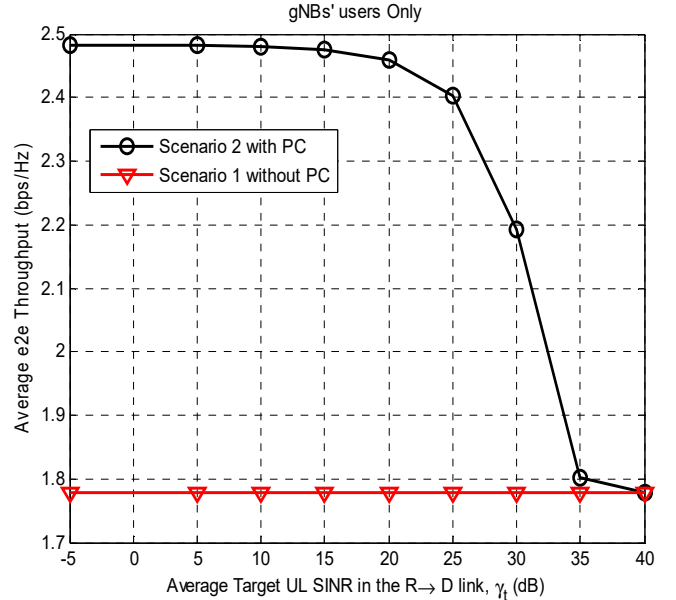

Fig. 7   Average e2e throughput for gNBs' UE only at different value of the UL SINR required in the $R \rightarrow D$ link, $\bar{\gamma}_t$

V.   CONCLUSION

In this paper, an efficient PC is proposed in order to mitigate the UL interference in 5G relay-based HetNets. Furthermore, the impact of PC at the RNs on the UL performance of 5G relay-based HetNets is investigated. Two scenarios are examined and compared: scenario 1 in which the PC at the RNs is not utilized and the proposed scenario 2 in which the PC at the RNs is utilized. Using UL PC at the RNs greatly improves the UL performance by reducing interference and increasing the average UL SINR and the average UL e2e throughput according to the simulations results. Simulation results also indicate that the users connected to gNBs benefit greatly from implementing UL PC at the RNs. This is due to the fact that the users of gNBs are greatly affected by the high interference created by the RNs' transmissions and using PC reduces RNs' transmission power

and interference during the second time slot which results in enhancing performance of UEs during the second time slot.

REFERENCES

[1] T. Q. Duong, X. Chu and H. A. Suraweera. "Ultra-dense networks for 5G and beyond: Modelling, analysis, and applications". John Wiley & Sons, Inc., 2019

[2] GSMA Association, "The mobile economy 2022". www.gsma.com. [Access date: July 2022].

[3] M. H. Alsharif and R. Nordin, "Evolution towards fifth generation (5G) wireless networks: Current trends and challenges in the deployment of millimetre wave, massive MIMO, and small cells," Telecommunication Systems, pp. 1-21, 2016.

[4] B. U. Kazi and G. Wainer. "Handover enhancement for LTE-Advanced and beyond heterogeneous cellular networks," 2017 International Symposium on Performance Evaluation of Computer and Telecommunication Systems (SPECTS), 2017, pp. 1-8, doi: 10.23919/SPECTS.2017.8046767.

[5] H. Z. Khan, M. Ali, I. Rashid, A. Ghafoor, M. Naeem, A. A. Khan, A. M. Saddiqui, "Resource allocation for energy efficiency optimization in uplink–downlink decoupled 5G heterogeneous networks," Wiley Int. J. Commun. Syst. doi: 10.1002/dac.4925. 2021 John Wiley & Sons Ltd.

[6] Yongjun Xu, Guan Gui,, Haris Gacanin , and Fumiyuki Adachi, "A survey on resource allocation for 5G heterogeneous networks: Current research, future trends, and challenges," IEEE Communications Surveys & Tutorials, vol. 23, no. 2, Second Quarter 2021. pp. 668 – 695.

[7] M. Tayyab, X. Gelabert, and R. Jäntti. "A survey on handover management: from LTE to NR," IEEE Access Journal, vol. 7, pp. 118907-118930, 2019.

[8] 3GPP, "Scenarios and requirements for small cell enhancements for E-UTRA and E-UTRAN (Release 12)," 3GPP Rep. TR 36.932 (V12.1.0), 3GPP, Sophia Antipolis, France, 2013.

[9] E. Gures, I. Shayea, A. Alhammadi, M. Ergen, and H. Mohamad. "A comprehensive survey on mobility management in 5G heterogeneous networks: Architectures, challenges and solutions," IEEE Access, vol. 8, pp. 195883- 195913, 2020.

[10] C. Yang, J. Li, M. Guizani, A. Anpalagan, and M. Elkashlan, "Advanced spectrum sharing in 5G cognitive heterogeneous networks," IEEE Wireless Commun., vol. 23, no. 2, pp. 94–101, Apr. 2016.

[11] M. U. A. Siddiqui, F. Qamar, F. Ahmed, Q. N. Nguyen, and R. Hassan, "Interference management in 5G and beyond network: Requirements, challenges and future directions," IEEE Access. vol. 9, 2021, pp. 68932–68965. doi: 10.1109/ACCESS.2021.3073543

[12] A. B. Mimoune and M. Kadoch, "Relay technology for 5G networks and IoT applications," in Internet of Things: Novel Advances and Envisioned Applications (Studies in Big Data), vol. 25, D. Acharjya and M. Geetha, Eds. Cham, Switzerland: Springer, 2017, doi: 10.1007/978-3-319-53472-5_1.

[13] S. Ranjan, P. Jha, P. Chaporkar and A. Karandikar, "A novel architecture for multihop relaying in 3GPP LTE and 5G networks," 2019 IEEE Conference on Standards for Communications and Networking (CSCN), pp. 1-6

[14] A. Kukushkin, "Introduction to mobile network engineering GSM, 3G-WCDMA, LTE and the road to 5G". John Wiley & Sons, Inc., 2018.

[15] A. Abrol and R. K. Jha, "Power optimization in 5G networks: A step towards green communication," IEEE Access, vol. 4, pp. 1355-1374, 2016.

[16] 3GPP, "3GPP TR 36.842 V12.0: "Study on small cell enhancements for E-UTRA and E-UTRAN; higher layer aspects," December 2013. [Online]. Available: http://www.3gpp.org/DynaReport/36-series.htm. [Accessed July 2022].

[17] J. Sultan, N. Misran, M. Ismail and M.T. Islam. "Topology-aware macro diversity handover technique for IEEE 802.16j multi-hop cellular networks". IET Communications Journal, vol. 5, no. 5, pp. 700-708,.2011.

[18] J. Sultan, N. Misran, M. Ismail & M.T. Islam. "A spectrally efficient macro diversity handover technique for interference-limited IEEE 802.16j multihop wireless relay networks," ETRI Journal, vol. 33, no. 4, pp. 558-568, 2011.

[19] R. Ahmed, E. A. Sundarajan, and A. Khalifeh. "A survey on femtocell handover management in dense heterogeneous 5G networks". Telecommunication System, vol. 75, pp 481-507, 2020.

[20] J. Sultan, M. Saif, N. Al-Thobhani, W. Abduljabbar,"Performance of Hrad Handover in 5G Heterogeneous Networks," 2021 1st International conference on Emerging Smart Technologies and applications, (eSmarTA 2021), pp. 1-7, doi: 10.1109/eSmarTA52612.2021.9515745.

[21] 3GPP, "3GPP TS 36.942 V16.0.0: Evolved Universal Terrestrial Radio Access (E-UTRA); Radio Frequency (RF) System Scenarios (release 16)" 2020-06. [Online]. Available: http://www.3gpp.org/DynaReport/36-series.htm. [Accessed July 2022].

[22] WINNER project, "IST-4-027756 WINNER II D 1.1.2 v1.0, WINNER II Channel Models," 2007.

[23] J. Conrat, Q. H. Chu, I. Maaz, and J. Cousin, "Path Loss Model Comparison for LTE-Advanced Relay Backhaul Link in Urban Environment. The 8th European Conference on Antennas and Propagation (EuCAP 2014), pp. 3472 – 3476.

[24] 3GPP, "3GPP TR 36.839 V11.1: Evolved Universal Terrestrial Radio Access (E-UTRA); Mobility enhancements in heterogeneous networks," 12 2012. [Online]. Available: http://www.3gpp.org/DynaReport/36-series.htm. [Accessed July 2022].

[25] K. Vasudeva, M. Simsek, D. López-Pérez and I. Guvenc, "Analysis of handover failures in heterogeneous networks with fading," IEEE Transaction on Vehicular Technology, vol. 66, no. 7, pp. 6060-6074, July 2017.

[26] A. Chiumento, M. Bennis, C. Desset, L. Van der Perre and S. Pollin, "Adaptive CSI and feedback estimation in LTE and beyond: a Gaussian process regression approach". EURASIP Journal on Wireless Communications and Networking, pp. 2 – 14. DOI 10.1186/s13638-015-0388-0.

[27] O. Oyman, J. N. Laneman, "Multihop relaying for broadband wireless mesh network: from theory to practice". IEEE Communication Magazine. Vol. 45 no. 11, pp. 116 – 122, 2007.

[28] S. Trankatwar, P. Wali, "Power control algorithm to improve coverage probability in heterogeneous networks," Wireless Personal Communication Journal, 2021. doi: 10.1007/11277-021-08739-y

[29] A. F. Isnawati, M. A. Afandi, "Performance analysis of game theoretical approach for power control system in heterogeneous network," International Journal of Intelligent Engineering & Systems, vol. 15, no. 3. 2022, pp. 397-405, doi: 10.22266/ijies2022.0630.33

[30] H. Ding, F. Zhao, J. Tian, D. Li, H.Zhang, "A deep reinforcement learning for user association and power control in heterogeneous networks,"Ad Hoc Network Journal, vol. 102, 2020, pp. 1-9

[31] Y. Lei, G. Zhu, C. Shen, Y. Xu, and X. Zhang,"Delay-aware user association and power control for 5G heterogeneous network," Mobile Nework and Apllication Journal, 2018, vol. 24, pp. 491-503, doi: 10.1007/s11036-018-1152-6.

[32] T. Zhou, Z. Liu, J. Zhao, C. Li, L. Yang, "Joint user association and power control for load balancing in downlink heterogeneous cellular networks," IEEE Trans. Veh. Technol., 2018, vol. 67, no. 3, pp. 2582-2593, doi: 10.1109/TVT.2017.2768574.

[33] X. Zhang, H. Zhao, J. Xiong, X. Liu, Li Zhou, J. Wei, "Scalable power control/beamforming in hetrogeneous network with graph neural networks," 2021 IEEE Global Communication Conference, 2021, doi: 10.1109/GLOBECOM46510.2021.9685457